

What Is the Representation of the Moisture–Tropopause Relationship in CMIP5 Models?*

YUTIAN WU

Department of Earth, Atmospheric, and Planetary Sciences, Purdue University, West Lafayette, Indiana

OLIVIER PAULUIS

Courant Institute of Mathematical Sciences, New York University, New York, New York, and New York University Abu Dhabi Institute, Abu Dhabi, United Arab Emirates

(Manuscript received 4 August 2014, in final form 17 March 2015)

ABSTRACT

A dynamical relationship that connects the extratropical tropopause potential temperature and the near-surface distribution of equivalent potential temperature was proposed in a previous study and was found to work successfully in capturing the annual cycle of the extratropical tropopause in reanalyses. This study extends the diagnosis of the moisture–tropopause relationship to an ensemble of CMIP5 models.

It is found that, in general, CMIP5 multimodel averages are able to produce the one-to-one moisture–tropopause relationship. However, a few biases are observed as compared to reanalyses. First of all, “cold biases” are seen at both the upper and lower levels of the troposphere, which are universal for all seasons, both hemispheres, and almost all CMIP5 models. This has been known as the “general coldness of climate models” since 1990 but the mechanisms remain elusive. It is shown that, for Northern Hemisphere annual averages, the upper- and lower-level “cold” biases are, in fact, correlated across CMIP5 models, which supports the dynamical linkage. Second, a large intermodel spread is found and nearly half of the models underestimate the annual cycle of the tropopause potential temperature as compared to that of the near-surface equivalent potential temperature fluctuation. This implies the incapability of the models to propagate the surface seasonal cycle to the upper levels. Finally, while reanalyses exhibit a pronounced asymmetry in tropopause potential temperature between the northern and southern summers, only a few CMIP5 models are able to capture this aspect of the seasonal cycle because of the too dry specific humidity in northern summer.

1. Introduction

The question of what determines the extratropical tropopause height is of fundamental importance to the general circulation of the atmosphere. It is generally believed that the height of the tropopause is controlled by both the radiative constraint from the stratosphere and the dynamical constraint stemming from the dry baroclinic instability in the tropospheric midlatitudes (Held

1982). Recent studies have also indicated the importance of the stratospheric large-scale dynamics (e.g., Birner 2010) and the tropospheric moist dynamics (Jukes 2000; Frierson et al. 2006; Frierson 2008; Korty and Schneider 2007; Schneider and O’Gorman 2008; Frierson and Davis 2011; Czaja and Blunt 2011) in regulating the tropopause.

A recent study of Wu and Pauluis (2014) further emphasized the role of low-level moisture and related the potential temperature of the extratropical tropopause to the near-surface distribution of equivalent potential temperature. The work was built upon the moist isentropic streamfunction, which is approximated based on the methodology of the statistical transformed Eulerian mean (Pauluis et al. 2011). Adopting a similar approach to Schneider (2004) but on moist isentropic streamfunction, Wu and Pauluis (2014) identified the tropopause based on the assumption that 90% of the equatorward mass flux within the surface layer is

* Supplemental information related to this paper is available at the Journals Online website: <http://dx.doi.org/10.1175/JCLI-D-14-00543.s1>.

Corresponding author address: Yutian Wu, 550 Stadium Mall Drive, Department of Earth, Atmospheric, and Planetary Sciences, Purdue University, West Lafayette, IN 47907.
E-mail: wu640@purdue.edu

balanced by the poleward mass flux taking place within the troposphere below the tropopause. It turns out that the equivalent potential temperature surface that accounts for 90% of the poleward moving mass flux ($\theta_{e, \text{pf}}$), or at which the tropopause is located (θ_{tp}), is reached where $\theta_{e, \text{pf}}$ is approximately equal to the mean plus two standard deviations of the near-surface equivalent potential temperature ($\theta_{e, \text{sfc}}$), that is,

$$\overline{\theta_{\text{tp}}} \approx \overline{\theta_{e, \text{pf}}} \approx \overline{\theta_{e, \text{sfc}}} + 2\overline{\theta_{e, \text{sfc}}^2}^{1/2}. \quad (1)$$

Here bars denote time and zonal averages and primes denote deviations from time and zonal averages, and subscripts tp, pf, and sfc represent tropopause, poleward-moving flow, and surface, respectively.

This moisture–tropopause relationship as in Eq. (1), in fact, indicates that it is the large and rare fluctuations of low-level equivalent potential temperature that are able to rise to the tropopause level and further modulate the tropopause potential temperature. In general, it is expected that the larger the fluctuation of low-level θ_e , the larger the tropopause potential temperature. This moisture–tropopause relationship is in qualitative agreement with Jukes (2000), where they empirically related the moist static stability to half the standard deviation of equivalent potential temperature. Our work differs from Jukes (2000) in that we compute the standard deviation of equivalent potential temperature rather than assuming that proportional to the meridional gradient of equivalent potential temperature. In Wu and Pauluis (2014), Eq. (1) was found to successfully capture the annual cycle of the extratropical tropopause in both the Northern and Southern Hemispheres, robust among different reanalyses. As discussed in Wu and Pauluis (2014), the annual cycle of the extratropical tropopause is largely dominated by that of the near-surface mean equivalent potential temperature; however, the eddy contributions also have a direct influence on extratropical tropopause, especially in northern summer. Furthermore, the proposed mechanism also works well in obtaining the interannual variability of the extratropical tropopause in northern summer. T. Schneider (2014, personal communication), however, claims that relationship (1) does not hold in the warm simulations of Schneider and O’Gorman (2008) that use a general circulation model with an idealized convection scheme and radiative transfer to simulate the climate on an aquaplanet with no annual cycle.

In this paper we extend the diagnosis of the dynamical relationship between the extratropical tropopause potential temperature and the near-surface equivalent potential temperature distribution to an ensemble of coupled climate models that participated in the Coupled Model Intercomparison Project phase 5 (CMIP5). In particular, we

aim to explore whether the dynamical relationship works for CMIP5 models and whether the low-level equivalent potential temperature distribution is able to capture the annual cycle of the extratropical tropopause.

It was recognized back to the IPCC First Assessment Report in 1990 that general circulation models tended to systematically simulate a colder temperature than that of observations and the cold temperature bias was most pronounced in the upper troposphere poleward of 50° latitude in both hemispheres and, to a lesser extent, in tropical and midlatitude lower troposphere (Houghton et al. 1990; Boer et al. 1992). This problem of the general coldness of climate models still remains in the state-of-the-art models that participated in the Fourth and Fifth Assessment Reports [e.g., see Fig. 1 of John and Soden (2007), Fig. 4 of Reichler and Kim (2008), and Fig. 2 of Charlton-Perez et al. (2013)]. However, the underlying reasons for this cold bias remain elusive and possible mechanisms have been proposed such as deficiencies in model physics and vertical resolution. A theoretical explanation was raised by Johnson (1997) from the perspective of entropy balance. Johnson (1997) argued that, in order to simulate a climate state without drift, positive definite nonphysical entropy sources introduced by numerical dispersion/diffusion and other reasons have to be offset through increased infrared cooling, which was believed to cause the “general coldness” in model simulations. It was also suggested in Johnson (1997) that this problem of cold biases could be eliminated in models of isentropic coordinates where nonphysical sources of entropy through numerical diffusion vanish. Studies such as Schaack et al. (2004) and Chen and Rasch (2012) used hybrid isentropic coordinates and found somewhat reduced cold biases in temperature in the upper troposphere and lower stratosphere. However, it is worth noticing that the cold biases in these studies largely remained, which suggests that other factors might also matter. This problem of the general coldness of climate models has a lot of consequences and, for example, is associated with biases in simulated atmospheric general circulation. Equatorward biases exist in the climatological jet position across different models; even worse, they could further affect the extent of the jet shift to external forcings in the future climate. As found in Kidston and Gerber (2010) and Son et al. (2010), in general, models of a more equatorward located climatological jet tend to move farther poleward in the late twenty-first century, which creates large uncertainties in the future projections of the jet shift. Therefore, it is important to better understand the underlying mechanisms of the cold biases in climate models. In this paper, from the perspective of the dynamical relationship in Eq. (1), we will discuss the

TABLE 1. CMIP5 models used in this study with information on host institute and atmospheric model resolution (L refers to number of vertical levels, T to triangular truncation, and C to cubed sphere).

Institute	Model name	Atmospheric resolution (lon × lat) level
Commonwealth Scientific and Industrial Research Organization (CSIRO), Australia, and Bureau of Meteorology (BOM), Australia	1. ACCESS1.0	N96 (1.875° × 1.25°) L38
	2. ACCESS1.3	N96 (1.875° × 1.25°) L38
Beijing Climate Center, China Meteorological Administration	3. BCC-CSM1.1	T42 (2.8125° × 2.8125°) L26
	4. BCC-CSM1.1-M	T106 (1.125° × 1.125°) L26
Beijing Normal University	5. BNU-ESM	T42 L26
	6. CanESM2	T63 (1.875° × 1.875°) L35
Canadian Centre for Climate Modeling and Analysis National Center for Atmospheric Research (NCAR)	7. CCSM4	288 × 200 (1.25° × 0.9°) L26
	8. CMCC-CESM	T31 (3.75° × 3.75°) L39
Centro Euro-Mediterraneo per I Cambiamenti Climatici	9. CMCC-CM	T159 (0.75° × 0.75°) L31
	10. CMCC-CMS	T63 L95
Centre National de Recherches Meteorologiques/Centre Europeen de Recherche et Formation Avancees en Calcul Scientifique	11. CNRM-CM5	T127 (1.4° × 1.4°) L31
	12. CSIRO-Mk3.6.0	T63 L18
Commonwealth Scientific and Industrial Research Organization in collaboration with the Queensland Climate Change Centre of Excellence	13. FGOALS-g2	128 × 60 (2.8125° × 3°) L26
	14. GFDL-CM3	C48 (2.5° × 2.0°) L48
LASG, Institute of Atmospheric Physics, Chinese Academy of Sciences; and CESS, Tsinghua University	15. GFDL-ESM2G	144 × 90 (2.5° × 2.0°) L24
	16. GFDL-ESM2M	144 × 90 (2.5° × 2.0°) L24
Geophysical Fluid Dynamics Laboratory (NOAA GFDL)	17. GISS-E2-R	144 × 90 (2.5° × 2.0°) L40
	18. INM-CM4	180 × 120 (2.0° × 1.50°) L21
NASA Goddard Institute for Space Studies (GISS) Institute for Numerical Mathematics	19. IPSL-CM5A-LR	96 × 96 (3.75° × 1.875°) L39
	20. IPSL-CM5A-MR	144 × 143 (2.5° × 1.25°) L39
Institut Pierre-Simon Laplace (IPSL)	21. IPSL-CM5B-LR	96 × 96 L39
	22. MIROC5	T85 143 (1.41° × 1.41°) L40
Japan Agency for Marine-Earth Science and Technology, Atmosphere and Ocean Research Institute (The University of Tokyo), and National Institute for Environmental Studies	23. MIROC-ESM	T42 L80
	24. MPI-ESM-LR	T63 L47
Max Planck Institute for Meteorology (MPI-M)	25. MPI-ESM-MR	T63 L95
	26. MRI-CGCM3	TL159 (1.1251° × 1.125°) L48
Meteorological Research Institute	27. NorESM1-M	144 × 96 (2.5° × 1.875°) L26
Norwegian Climate Centre		

possible dynamical linkage between the upper- and lower-level cold biases across CMIP5 models.

In this paper, we examine the annual cycle of the extratropical tropopause in an ensemble of CMIP5 models and how it is related to that of the near-surface equivalent potential temperature distribution. Biases, in comparison to reanalyses, will be discussed. This paper is organized as follows. Section 2 describes the reanalysis data and CMIP5 simulations used in this study. In section 3, the links between the annual cycle of the extratropical tropopause and that of the near-surface equivalent potential temperature distribution are discussed. Section 4 concludes the paper.

2. CMIP5 climate models

We make use of an ensemble of the latest generation of the coupled climate models that participated in phase

5 the Coupled Model Intercomparison Project phase 5 (Taylor et al. 2012). In this study, 27 coupled climate models from 17 modeling centers are used based on the availability of daily temperature and daily specific humidity. These models as well as their developing institutes and atmospheric model resolutions are listed in Table 1. Since the daily output of CMIP5 archive is only available on eight pressure levels (1000, 850, 700, 500, 250, 100, 50, and 10 mb), for the calculation of the near-surface $\bar{\theta}_e + 2\bar{\theta}_e^{1/2}$, daily temperature and specific humidity at 850 mb are used. Following Wu and Pauluis (2014), the extratropical tropopause is identified based on the definition of the dynamical tropopause where the potential vorticity is equal to 2 PVU. Monthly output of temperature on 17 standard pressure levels is used to identify the dynamical tropopause and its associated potential temperature because of the finer vertical resolution in the upper troposphere and lower stratosphere

in monthly output. To examine the annual cycle of the extratropical tropopause and its one-to-one correspondence with the low-level distribution of equivalent potential temperature, we estimate $\overline{\theta_{tp}}$ averaged in the 35°–45° latitude band and $\overline{\theta_e} + 2\overline{\theta_e^2}^{1/2}$ in the 25°–35° latitude band. The 10°-latitudinal shift represents the dynamical processes that connect the lower and upper levels of the atmosphere, which are not exactly upright but take place over a horizontal distance, on the order of the Rossby radius. And the 10°-latitudinal shift is not crucial for obtaining the one-to-one relationship of the annual cycle (Wu and Pauluis 2014). The r11p1 integration in the historical runs is used for each model (except for the r6i1p1 integration for GISS-E2-R) and the diagnosis is performed during 1980–99, the identical period as in Wu and Pauluis (2014) for the reanalyses.

As a reference, we make use of three reanalyses including the ERA-Interim reanalysis (Dee et al. 2011), the NCEP–DOE Reanalysis II (NCEP2; Kanamitsu et al. 2002), and the NCEP Climate Forecast System Reanalysis (CFSR; Saha et al. 2010). As shown in Wu and Pauluis (2014), these three reanalyses provide rather consistent results on both the annual cycle and interannual variability of the extratropical tropopause. Biases in CMIP5 integrations are identified as the difference between model integrations and the above three reanalyses.

3. Results in CMIP5 models

a. Annual cycle of extratropical tropopause and low-level moisture

As shown in Wu and Pauluis (2014), there is a one-to-one relationship between the extratropical tropopause potential temperature and the near-surface equivalent potential temperature distribution for all seasons and for both the two hemispheres. In other words, a large fluctuation of near-surface θ_e is always associated with a large value of upper-level θ_{tp} . In particular, the correlation between the two is very close to one, and the linear regression coefficient is above 0.8 for the NH annual cycle and is above 0.7 for the SH annual cycle. Therefore, similarly here we extend the diagnosis to an ensemble of CMIP5 models and quantitatively measure the dynamical relationship using the correlation coefficient and linear regression coefficient (LR) as well as the annual means of θ_{tp} and near-surface $\overline{\theta_e} + 2\overline{\theta_e^2}^{1/2}$.

First of all, Fig. 1a shows the moisture–tropopause relationship in CMIP5 multimodel averages in the NH. In comparison to the reanalysis datasets, the CMIP5 multimodel mean is able to successfully reproduce the one-to-one relationship between the low-level equivalent

potential temperature fluctuation and tropopause potential temperature with a close to unity correlation and linear regression coefficient (or slope). However, although the close-to-unity correlation is a robust feature among individual CMIP5 models, there is quite a spread in the modeled slope of the annual cycle (see the results of individual models in supplementary Figs. S1–S3, file JCLI-D-14-00543s1). This is also true for the SH (see Fig. 2a and Figs. S4–S6).

Figure 3 shows the modeled slope for the 27 CMIP5 models and for both the two hemispheres. As mentioned above, the slope of the annual cycle varies a lot from model to model—the NH slope ranges from 0.6 to 1.05 while the SH slope covers from 0.5 to 0.85. The modeled slopes of the two hemispheres are slightly correlated (with a correlation of 0.39, which is statistically significant at the 95% confidence level), which suggests that models that do poorly in one hemisphere tend to perform poorly in the other hemisphere as well. As mentioned in section 2, we group together three reanalysis datasets including ERA-Interim, NCEP2, and CFSR. The confidence interval is constructed by using the bootstrap method, which independently resamples the results with replacement, each time a new slope is calculated using the new samples, and repeating for a large number of times. As shown in Fig. 3, the confidence interval is calculated as the 2.5th and 97.5th percentiles of these new slopes from each resampling (similarly for the confidence intervals in other figures). Therefore, depending on how the modeled slope is compared to the constructed confidence interval, the 27 CMIP5 models can be divided into three groups that have smaller, similar, and larger slopes, all statistically significant at the 95% confidence level.

For the NH, group N1 has 12 CMIP5 models that have smaller linear regression coefficients than that of the reanalyses, group N2 is characterized by a similar annual cycle slope to that of the reanalyses and includes 14 models, and only one model has a larger linear regression coefficient and is included in group N3. A list of the models in N1, N2, and N3 is given in Table 2. Similarly, for the SH, group S1 includes 16 models with smaller linear regression coefficients, and the other 11 models have similar slopes and are included in group S2 (Table 2). Figures 1b–d show the moisture–tropopause relationship for groups N1, N2, and N3, respectively; Figs. 2b and 2c do the same for S1 and S2.

In addition to the slope of the annual cycle, another striking feature in CMIP5 model simulations is the systematic cold bias in both the near-surface equivalent potential temperature fluctuation and the tropopause potential temperature. This will be further discussed in the next subsection.

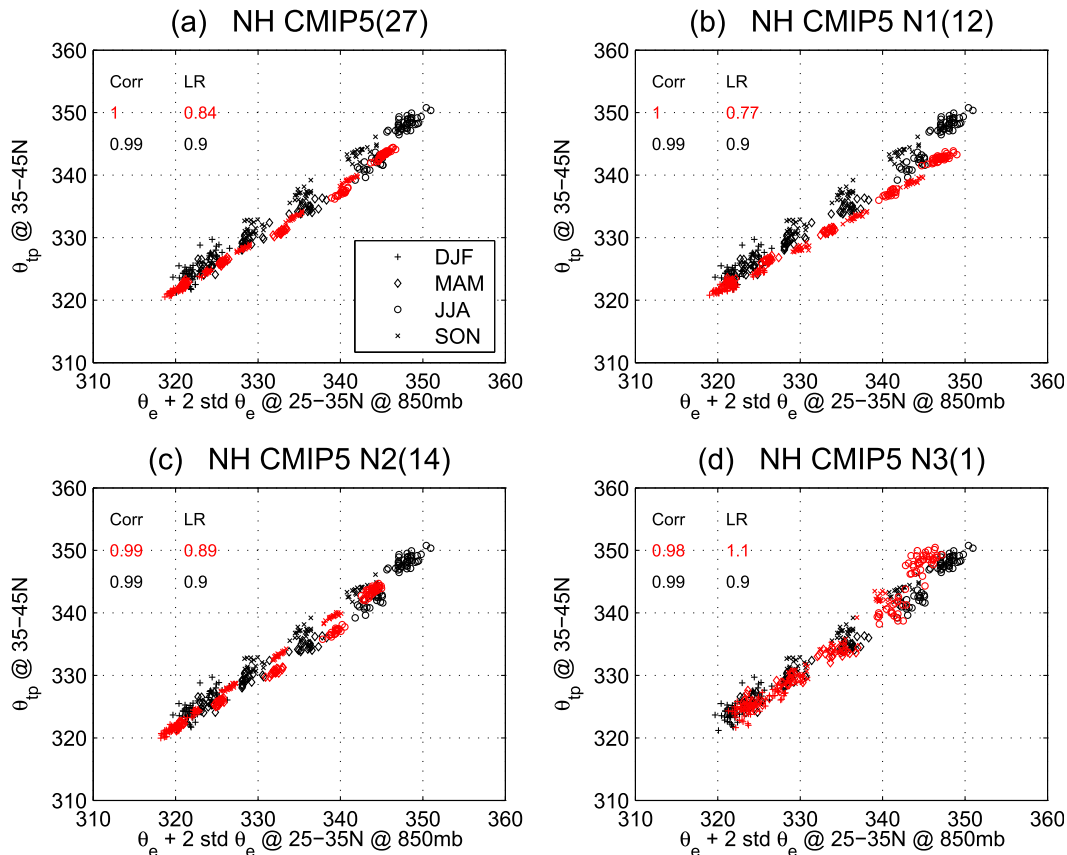


FIG. 1. The seasonal cycle of the dynamical relationship between $\overline{\theta_e + 2\overline{\theta_e}^2/2}$ averaged over 25°–35°N at 850 mb and θ_{tp} averaged over 35°–45°N for multimodel averages of (a) all 27 CMIP5 models, (b) group N1 (includes 12 models), (c) group N2 (includes 14 models), and (d) group N3 (includes 1 model). Groups N1, N2, and N3 cover models with smaller, similar, and larger coefficients of linear regression compared to reanalyses, respectively. The results for the average of three reanalyses are shown in black symbols and those for CMIP5 models are shown in red symbols. The plus symbols correspond to December–February (DJF), diamond symbols to March–May (MAM), circles to June–August (JJA), and crosses to September–November (SON), as indicated in legend. The coefficients of correlation and linear regression are also shown.

The slope of the annual cycle is an important measure of the one-to-one moisture–tropopause relationship. However, as indicated in Fig. 3, nearly half of the models underestimate the slope of the moisture–tropopause annual cycle. In fact, the largest underestimation of the extratropical tropopause occurs in summer, which contributes to the underestimation of the annual cycle slope. For example, the underestimation of the slope in group N1 is largely because of the smaller near-surface $\theta_e + 2\overline{\theta_e}^2/2$ and even smaller extratropical θ_{tp} in northern summer, as shown in Fig. 1b. This further indicates that, even with similar values of low-level fluctuation of equivalent potential temperature after correcting the low-level “cold” biases, these CMIP5 models in group N1 still cannot achieve as large potential temperature at the extratropical tropopause as the reanalyses. In fact, even after an extrapolation of the

simulated annual cycle to achieve similar values of low-level θ_e to that of the reanalyses, the extratropical tropopause potential temperature in group N1 is still about 5–10 K “colder” than that of the reanalyses. This might imply possible issues with regard to the representation of moist processes in group N1, such as too much entrainment of dry air in convective updrafts, which would prevent the fluctuation of equivalent potential temperature near the surface to be transmitted into the upper troposphere. This behavior is distinct from groups N2 and N3 despite the similar systematic cold biases. It is noteworthy that the tropopause potential temperature in the N3 group is significantly larger than the surface fluctuation of equivalent potential temperature during summer (shown in Fig. 1d).

With these many climate models and distinct representations of moist processes, it is difficult to conclude

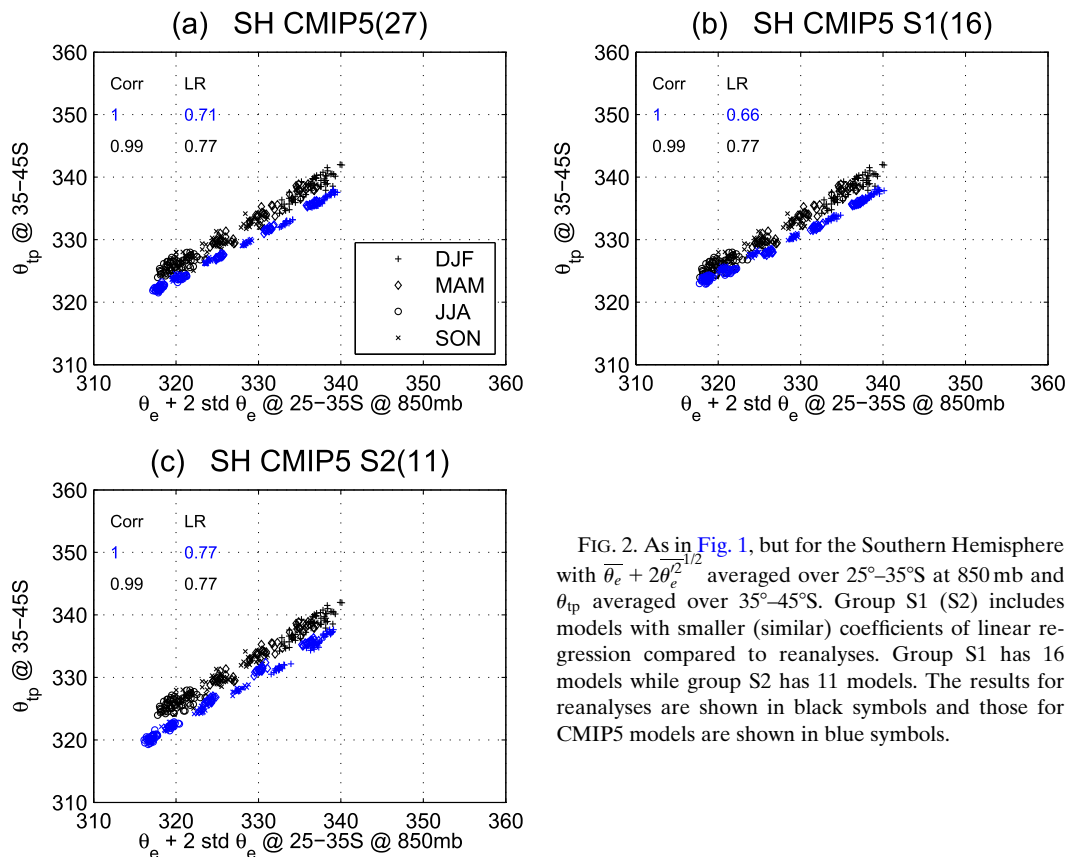


FIG. 2. As in Fig. 1, but for the Southern Hemisphere with $\theta_e + 2\theta_e^{1/2}$ averaged over $25^\circ\text{--}35^\circ\text{S}$ at 850 mb and θ_{tp} averaged over $35^\circ\text{--}45^\circ\text{S}$. Group S1 (S2) includes models with smaller (similar) coefficients of linear regression compared to reanalyses. Group S1 has 16 models while group S2 has 11 models. The results for reanalyses are shown in black symbols and those for CMIP5 models are shown in blue symbols.

what exactly is problematic in groups N1 and N3. However, we believe that these discrepancies arise in part due to the inadequate dynamics or physics in climate models. While the ability of cumulus parameterization has been recognized as a significant challenge for the modeling of the tropical climate, our study suggests that similar deficiencies in the representation of moist processes also negatively impact the higher latitudes. The dynamical relationship between the surface and the tropopause could offer a straightforward approach to diagnose such issues in a range of climate models. More detailed sensitivity experiments are needed for a thorough understanding of the mechanisms and we leave that for future work.

b. Systematic “cold” biases

As shown in Figs. 1 and 2, coupled climate models tend to produce systematic cold biases in both the near-surface equivalent potential temperature distribution and the upper-level potential temperature in the extratropics for all seasons and for both hemispheres. This is consistent with the phenomenon of the general coldness of climate models, which is a long-standing problem since the IPCC First Assessment Report in 1990.

Johnson (1997) suggested that the general coldness arises from numerical dispersion–diffusion and resulting positive definite nonphysical entropy sources, and thus is likely intrinsic to climate models. Efforts were made using other model coordinates, and cold biases in upper-level temperature were, to some extent, reduced but still retained (e.g., Schaack et al. 2004; Chen and Rasch 2012). Here we further look into the cold biases in the upper-level potential temperature across CMIP5 models and investigate their possible linkage to the cold biases in the near-surface equivalent potential temperature distribution.

Here we focus on the annual averages in NH extratropics, and the intermodel spread as well as the result from reanalyses is shown in Fig. 4. It can be seen that the majority of the CMIP5 models tends to produce cold biases at both the upper and lower levels. Here the term “cold biases” refers to, in comparison to that of reanalyses, smaller θ or θ_e values, not necessarily only cold biases in temperature. Furthermore, it is found that the upper- and lower-level cold biases are correlated across CMIP5 models, with a correlation of 0.56. This suggests that the cold biases at the upper and lower levels of the NH extratropics might be indeed dynamically

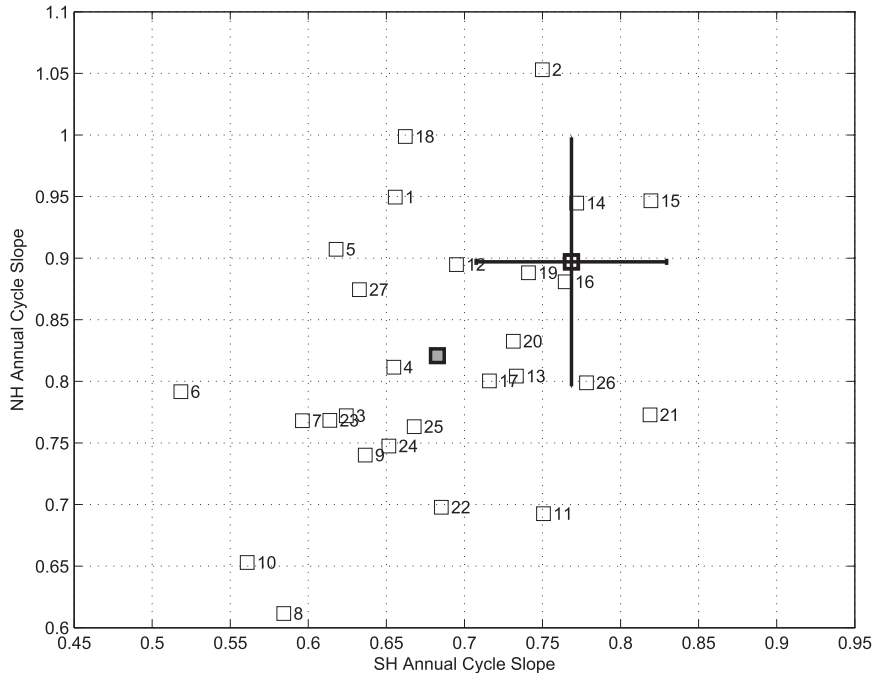


FIG. 3. The CMIP5 slopes of the annual cycle of the moisture–tropopause relationship for the Northern and Southern Hemispheres. The reanalyses are plotted in a thick square with the error bars showing the confidence intervals (see text for more details). The model results are plotted in thin squares with the numbers indicating the model numbers as in Table 1 and the multimodel mean is plotted as a thick gray square.

connected, and models with a colder bias at lower levels tend to have a colder bias at the extratropical tropopause.

Although the focus of this study is the overall performance of CMIP5 models, it is probably worth noticing that, for NH annual averages, two of the farthest outliers are the IPSL-CM5A-LR (model 19) and the IPSL-CM5B-LR (model 21), which are from the same modeling center. For the annual cycle of the NH extratropical tropopause, the IPSL-CM5B-LR performs quite differently from the IPSL-CM5A-LR, and the former has a smaller coefficient of linear regression and deviates farther away from the reanalyses (see Fig. S3). In comparison to IPSL-CM5A-LR, the IPSL-CM5B-LR includes a new version of the physical package and boundary layer parameterization as well as a modified deep convection scheme (Hourdin et al. 2013). As a result, improvements are found in this new version model in the better representation of the convective boundary layer, the cumulus clouds, the diurnal cycle of deep convection over continents, and a Madden–Julian oscillation (MJO)–like signal in the tropics. However, as also demonstrated in Hourdin et al. (2013), significant biases still remain and some are even amplified in this new model version such as a stronger cold bias in tropospheric temperature and a more equatorward located jet

stream. This is consistent with what we find here: despite a small improvement in the low-level equivalent potential temperature distribution, the extratropical tropopause potential temperature is even colder in IPSL-CM5B-LR (i.e., as shown in Fig. 4, θ_{tp} in IPSL-CM5B-LR is about 2 K colder than IPSL-CM5A-LR and is about 8 K colder than the reanalyses). It is also noticed that IPSL-CM5A-MR (model 20), the old model version but with finer horizontal resolution, behaves better than both the IPSL-CM5A-LR and IPSL-CM5B-LR. Furthermore, we have

TABLE 2. CMIP5 groups: N1, N2, and N3, with the modeled slope of the Northern Hemisphere moisture–tropopause annual cycle smaller, similar, and larger compared to reanalyses, respectively; similarly for S1 and S2. The numbers within the parentheses indicate the models belonging to that group and are sorted out on the order of ascending slope values. See Table 1 for a list of the models.

Northern Hemisphere	
Group	Models
N1 (12)	8, 10, 11, 22, 9, 24, 25, 7, 23, 3, 21, 6
N2 (14)	26, 17, 13, 4, 20, 27, 16, 19, 12, 5, 14, 15, 1, 18
N3 (1)	2
Southern Hemisphere	
Group	Models
S1 (16)	6, 10, 8, 7, 23, 5, 3, 27, 9, 24, 4, 1, 18, 25, 22, 12
S2 (11)	17, 20, 13, 19, 11, 2, 16, 14, 26, 21, 15

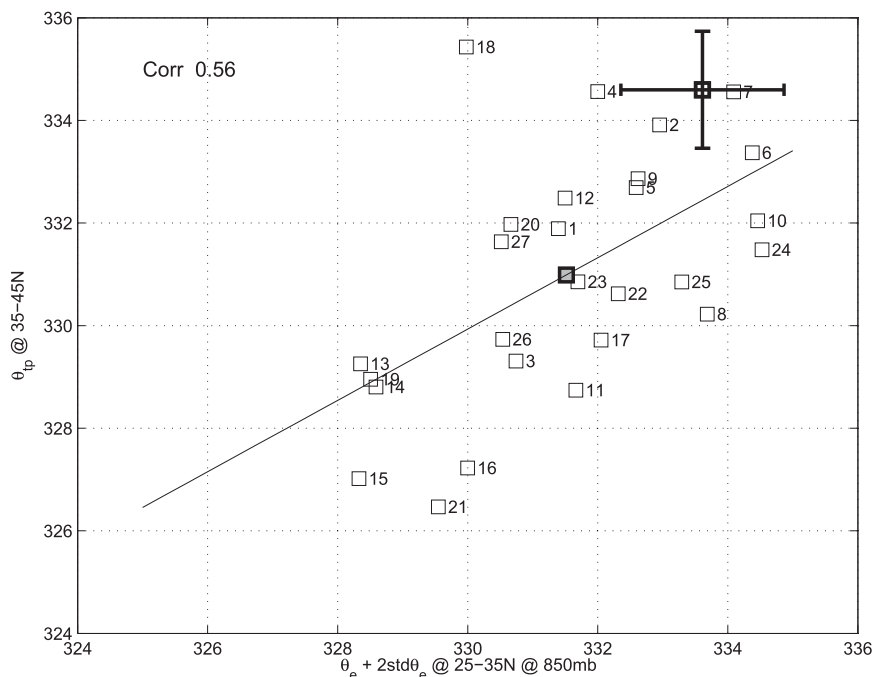


FIG. 4. The Northern Hemisphere annual mean $\overline{\theta_e} + 2\overline{\theta_e}^{1/2}$ at 850 mb averaged over 25°–35°N vs the annual mean θ_{tp} averaged over 35°–45°N for 27 CMIP5 models. The results from reanalyses are plotted in a thick empty square with the error bars showing the confidence intervals (constructed in a similar way to Fig. 3). The CMIP5 results are plotted in thin empty squares and the multimodel average is shown in a thick gray square. A correlation of 0.56 is found across the models and a linear regression is also plotted as a black line.

found that models with a finer horizontal resolution, in general, tend to perform better than those with a coarser resolution (not shown), which is in agreement with the performance of the IPSL models.

Figure 5a further examines the cold biases in the near-surface equivalent potential temperature distribution and separates that into the contributions from time mean and eddy biases. There is almost no correlation between the simulation of the mean state and that of the eddies across models (the correlation is about 0.16 and is not statistically significant at the 95% confidence level). While CMIP5 multimodel averages can produce more or less similar values of standard deviations of equivalent potential temperature, most of the models systematically underestimate the time mean values of equivalent potential temperature. Figure 5b further attributes the cold biases in mean θ_e into the contributions from θ and $\theta_e - \theta$, which approximately measures cold–warm biases in temperature and dry–moist biases in specific humidity, respectively. It can be seen that for majority of the models, the cold biases in near-surface θ_e result from both the colder temperature and drier specific humidity, with a small correlation (0.38, which is statistically significant at the 95% confidence level) between the two across models. This is also a common

deficiency as found in CMIP3 models, where the simulated temperatures were systematically colder throughout the troposphere and the specific humidity was drier in the lower troposphere (e.g., John and Soden 2007). It is noted here that both the cold bias in temperature and dry bias in relative humidity could contribute to the dry bias in near-surface $\theta_e - \theta$. A multimodel plot of near-surface relative humidity in NH subtropics can be found in Fig. S7. A rather large intermodel spread is observed among the CMIP5 models although the multimodel mean shows a dry bias in relative humidity ($\sim 2\%$). In the multimodel mean, the dry bias in $\theta_e - \theta$ is largely due to the cold bias in temperature and, to a lesser extent, the dry bias in relative humidity. Therefore, it is both the cold bias in temperature and the dry bias in specific humidity in CMIP5 models that contribute to the cold bias in the near-surface distribution of equivalent potential temperature, which is further related to the cold bias in the upper-level potential temperature at the extratropical tropopause.

We notice that the cold biases in zonal mean temperature are more prominent in the polar lower stratosphere, as can be found in Fig. 1 of John and Soden (2007), Fig. 4 of Reichler and Kim (2008), and Fig. 2 of Charlton-Perez et al. (2013). But since the maxima of

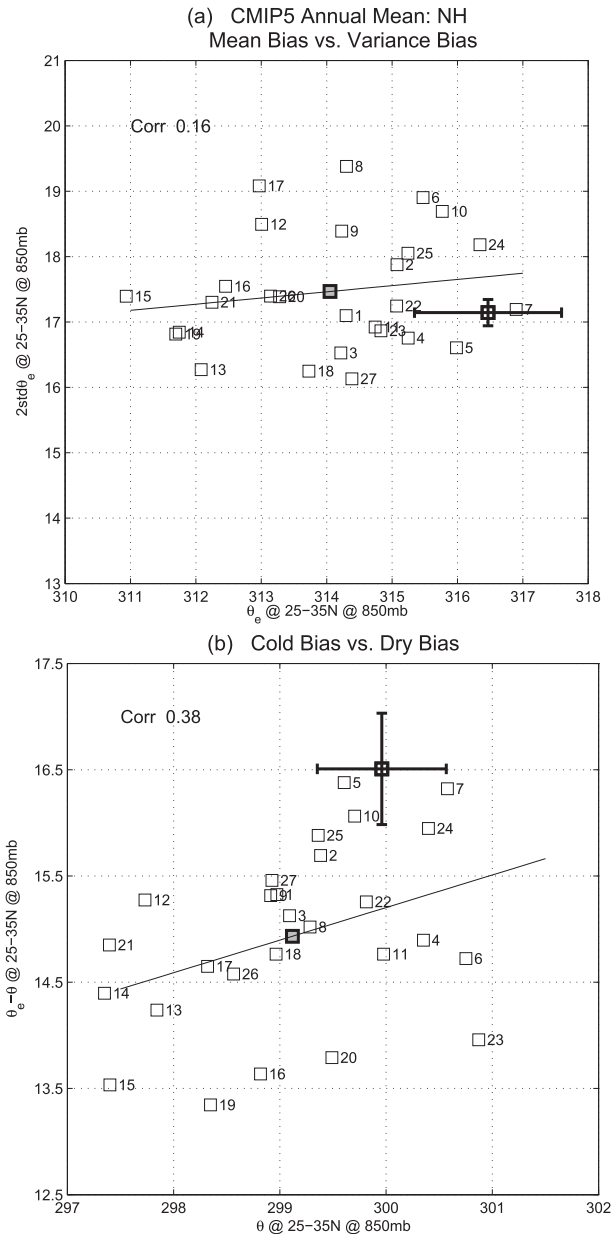


FIG. 5. (a) The Northern Hemisphere annual mean θ_e vs the annual mean $2\theta_e^{2/3}$, both at 850 mb averaged over 25°–35°N, for 27 CMIP5 models. (b) As in (a), but for θ vs $\theta_e - \theta$. The results from reanalyses are plotted in thick empty squares with the error bars showing the confidence intervals. The CMIP5 results are plotted in thin empty squares and the multimodel average is shown in a thick gray square. A correlation of 0.16 and 0.38 is found across the models for (a) and (b), and a linear regression is also plotted in black.

cold biases are located above the tropopause level, we speculate that they are not directly related to near-surface biases.

The SH annual averages across CMIP5 models are slightly different from the NH and the intermodel

spread is less organized (not shown). In particular, the cold biases at the upper and lower troposphere are less correlated with a correlation coefficient of 0.38. In the next subsection, we will discuss more about the different behaviors in the two hemispheres.

c. Hemispheric asymmetry in summertime extratropical tropopause and low-level moisture

The summer temperature is higher in the NH than in the SH due to the asymmetric distribution of continents. During the summer months, land temperature increases more rapidly than the ocean temperature due to the lower heat capacity of land. This warming is transferred to the entire atmospheric column; as a result, the tropopause potential temperature is higher in northern summer than in southern summer. This asymmetry between the two summers can be seen in the reanalyses shown in Fig. 6a; the northern summer is about 10 K warmer at both the upper and lower troposphere than the southern summer.

Here we only estimate the near-surface equivalent potential temperature and the extratropical tropopause potential temperature at the 25°–35° and 35°–45° latitude bands, respectively, but the large asymmetry is also true for the whole hemispheric average and the northern summer is warmer because of the greater land fraction in the NH (see Figs. 1 and 2 of Kang et al. 2015). In fact, the warmer northern summer further leads to a warmer NH in the annual average than the SH, which potentially has important implications for the position of the intertropical convergence zone and the tropical rainfall belt (Kang et al. 2008). Therefore, it is important that climate models produce the right amount of hemispheric asymmetry.

Figure 6a shows the dynamical relationship in northern summer averages and in southern summer averages across 27 CMIP5 models. As can be seen, in northern summer, the majority of the CMIP5 models underestimate both the tropopause potential temperature and the near-surface distribution of equivalent potential temperature, which is known as the general coldness of climate models. In fact, the largest cold biases in multimodel averages occur in northern summer. In southern summer, while a large number of models also underestimate the tropopause potential temperature, the simulation of near-surface equivalent potential temperature distribution across models is rather scattered.

Figure 6b shows the difference between northern summer and southern summer for reanalyses and models. By taking the difference between the two summers, one can remove the global cold bias and better capture the difference in annual cycle over land and ocean. It can be seen that a large part of models underestimates the asymmetry between the two summers,

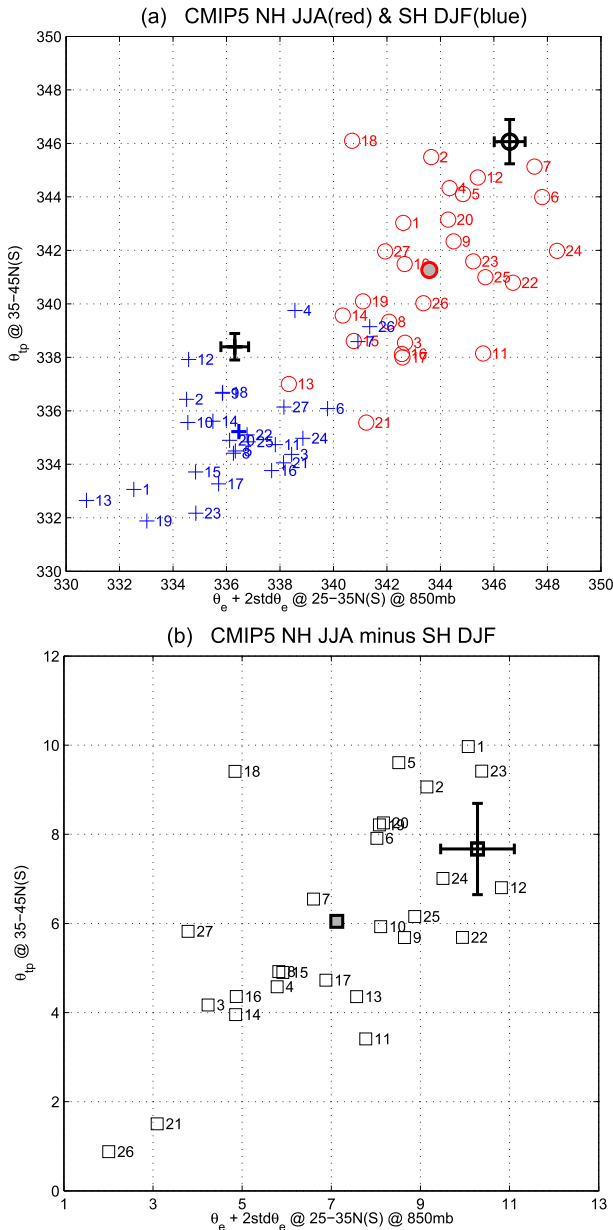


FIG. 6. (a) The dynamical relationship for NH summer (indicated by red circles) and for SH summer (indicated by blue crosses) for CMIP5 models. (b) The difference between NH and SH summer for CMIP5 models (thin empty squares). The results for the re-analyses are shown as a reference with a thick black square. The CMIP5 multimodel average is plotted in thick red and thick blue in (a) and by a thick gray square in (b).

by about 3K at the lower level and about 2K at the upper level in multimodel averages.

To further examine the lack of asymmetry at lower levels, Fig. 7a separates that into the contributions from time mean and eddy components of equivalent potential temperature. It is found that it is mainly the

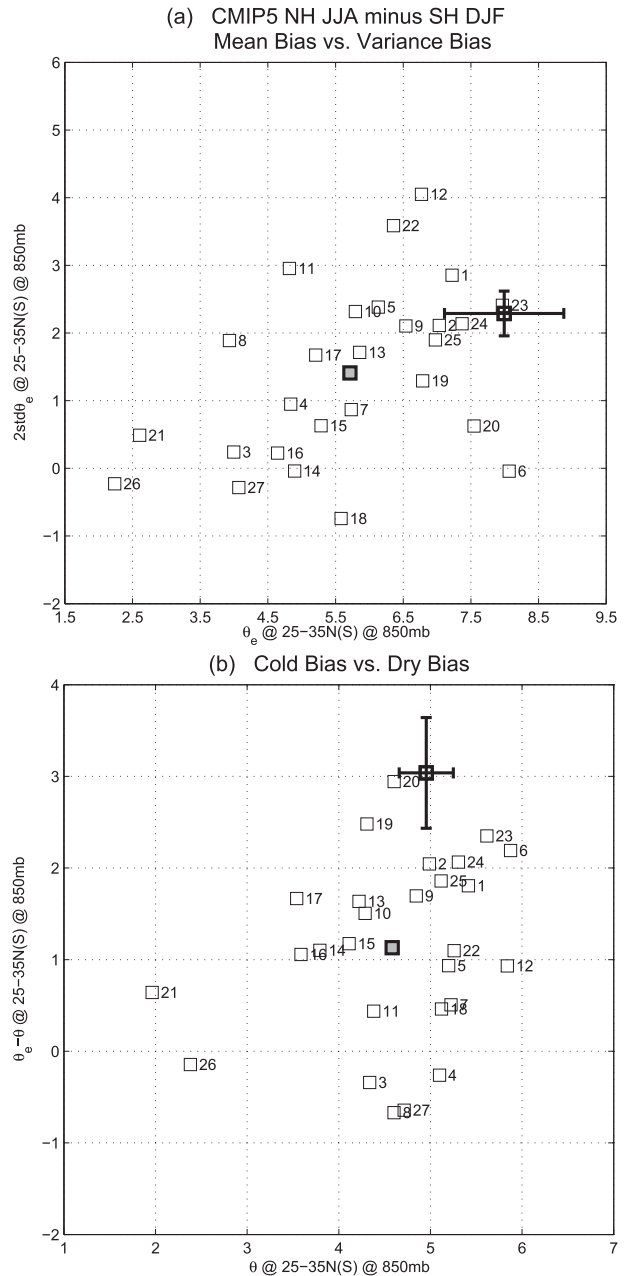


FIG. 7. The difference between NH JJA and SH DJF in (a) time-mean θ_e vs $2\overline{\theta_e^2}^{1/2}$, both averaged over 25° – 35° latitude at 850mb, and (b) time-mean θ vs $\theta_e - \theta$, for 27 CMIP5 models. The results from the reanalyses are shown as a reference in a thick empty square. The CMIP5 results are plotted with thin empty squares with the multimodel average in a thick gray square.

underestimation of the mean θ_e in northern summer relative to southern summer that contributes to the lack of asymmetry at lower levels. In addition, to a lesser extent, more than half of the models also fail to produce the correct amount of hemispheric difference in the eddy component, and a few models even get the wrong

sign. Furthermore, Fig. 7b separates the lack of asymmetry in time mean equivalent potential temperature into that of the dry (θ) and moist ($\theta_e - \theta$) components. While the simulations of the low-level θ are scattered, most of the models systematically fail to produce the 3-K hemispheric asymmetry in the moisture component. This indicates that, in comparison to southern summer, the northern summer is systematically too dry in specific humidity at lower levels, which results in a reduced amount of fluctuations of equivalent potential temperature. As a result, the subtropical low-level air parcels are less energetic in model simulations and are less able to rise to the tropopause level and to modulate the tropopause potential temperature.

Therefore, it is found here that in reanalyses a large asymmetry exists in both the upper and lower troposphere, with the northern summer about 10 K warmer than the southern summer. However, coupled climate models systematically underestimate this hemispheric asymmetry by about 3–4 K. This lack of asymmetry at lower levels largely comes from the fact that the simulated northern summer is too dry in time-mean specific humidity, which reduces the low-level fluctuations of moisture. This underestimation of low-level moisture in northern summer is further related to the upper-level potential temperature via moist dynamical processes, and as a result the simulated extratropical tropopause is too cold in northern summer relative to southern summer, leading to an underestimation of hemispheric asymmetry in extratropical tropopause potential temperature. Therefore, a model's incapability to reproduce the summer asymmetry is often tied to its incapability to capture the large equivalent potential temperature during northern summer.

4. Discussion and conclusions

This study diagnoses the dynamical relationship that connects the extratropical tropopause potential temperature to the near-surface equivalent potential temperature distribution using an ensemble of CMIP5 coupled climate models. This moisture–tropopause relationship, in fact, pictures the midlatitude moist processes that carry the subtropical low-level poleward-moving air parcels upward and poleward to the extratropical tropopause. As in Wu and Pauluis (2014), a one-to-one relationship was found between the near-surface equivalent potential temperature distribution and the extratropical tropopause potential temperature for the annual cycle, which is a robust feature among different reanalyses. The annual cycle is characterized by a correlation coefficient very close to one and also a slope close to one, which is above 0.8 for the NH and

above 0.7 for the SH. In this study, with 27 climate models from the CMIP5 archive, we explore the representation of the extratropical tropopause annual cycle, and in particular examine whether these state-of-the-art models are able to capture the one-to-one relationship between the upper and lower levels. For reference, three reanalyses (ERA-Interim, NCEP2, and CFSR) are used.

Here we summarize the findings:

- In general, CMIP5 multimodel averages are able to produce the one-to-one dynamical relationship between the near-surface equivalent potential temperature distribution and the extratropical tropopause potential temperature for both the Northern and Southern Hemispheres. The correlation coefficient is very close to one and the linear regression coefficient is largely similar to that of the reanalyses. However, “cold” biases are seen at both the upper and lower levels and are universal for all seasons and for both the two hemispheres, systematically for all CMIP5 models. This general coldness of climate models is a long-standing issue dated back to the IPCC First Assessment Report in 1990 and still remains.
- Looking into individual models, a large intermodel spread is found and a large part of CMIP5 models underestimates the slope of the dynamical relationship for the annual cycle. The smaller slope is mostly due to the underestimation of the extratropical tropopause potential temperature in northern (NH) summer [June–August (JJA)] and in southern (SH) summer [December–February (DJF)]. This indicates that, in some model simulations, even with similar values of equivalent potential temperature, the low-level air parcels are not able to rise to the extratropical tropopause level. This might suggest possible issues regarding the representation of the moist processes in the subtropical and midlatitude regions in some models.
- The systematic cold biases in CMIP5 models are further investigated, in particular in Northern Hemisphere annual averages. It is found that the cold biases in near-surface equivalent potential temperature and in extratropical tropopause potential temperature are correlated across the 27 CMIP5 models. In general, models with a colder bias at the lower level tend to have a colder bias at the upper level as well. In addition, the cold biases in near-surface equivalent potential temperature distribution are largely a result of cold biases in temperature and dry biases in specific humidity at lower levels. It is noted here that, in general, models with a finer horizontal resolution as a whole appear to have smaller cold biases at both

the upper and lower levels than those with a coarser resolution.

- As mentioned above, the underestimation of the annual cycle is largely due to the poor representations of the northern summer and the southern summer. While the reanalyses show a large asymmetry between the two summers with about 10 K larger values of near-surface equivalent potential temperature and extratropical tropopause potential temperature in northern summer, a large part of models fails to produce the hemispheric asymmetry by about 3–4 K. In comparison to southern summer, the northern summer is found to be too dry in mean specific humidity, which leads to reduced fluctuations of low-level equivalent potential temperature and extratropical tropopause potential temperature.

The annual cycle of the extratropical tropopause is largely dominated by the near-surface mean equivalent potential temperature, which can be partially understood from radiative constraints as in previous studies (e.g., Held 1982; Thuburn and Craig 2000; Schneider 2007). However, the fact that the relationship (1) relates the surface equivalent potential temperature to the extratropical tropopause temperature emphasizes the importance of moist processes for the maintenance of the extratropical tropopause. The contribution from the eddy component, is however also significant, especially in northern summer, and will be discussed in a follow-up paper.

This study applies the dynamical relationship proposed in Wu and Pauluis (2014) to an ensemble of CMIP5 models—in particular, the representation of the annual cycle. The good correlation in both reanalyses and CMIP5 models, as seen in Figs. 1 and 2, is largely due to the dominance of the annual cycle. In the annual cycle, links between the upper and lower troposphere are also seen in model simulations and they might, in fact, suggest possible solutions to the deficiencies of model simulations. For example, as for the problem of the general coldness of climate models, perhaps a finer horizontal resolution or/and a better representation of the boundary layer temperature and humidity distribution might help reduce the cold biases at upper troposphere lower stratosphere. In addition, we believe that the diagnosis using the dynamical relationship is a good and easy way to examine the subtropical and midlatitude moist processes in a group of climate models, and in particular to explore whether the moist convection schemes or large-scale dynamics are successful or not in representing the moist processes. More parameter sensitivity experiments are needed to further explore how the dynamical relationship varies with parameters in the moist convection schemes. This will help better interpret the CMIP5 results and will

lead to an improved understanding and representation of moist dynamical processes.

Acknowledgments. The authors thank Prof. Tapio Schneider and two anonymous reviewers for constructive comments on the manuscript. We are also thankful to the useful comments from Prof. David Raymond during the 19th Conference on Atmospheric and Oceanic Fluid Dynamics. We also acknowledge the World Climate Research Programme's Working Group on Coupled Modelling, which is responsible for CMIP, and we thank the climate modeling groups (listed in Table 1 of this paper) for producing and making available their model output. For CMIP the U.S. Department of Energy's Program for Climate Model Diagnosis and Intercomparison provides coordinating support and led development of software infrastructure in partnership with the Global Organization for Earth System Science Portals. YW and OMP have been supported by the NSF under Grant AGS-0944058 for this work. YW also acknowledge the support from a startup fund from the Department of Earth, Atmospheric, and Planetary Sciences at Purdue University. OMP has also been supported by the NYU Abu Dhabi Institute under Grant G1102.

REFERENCES

- Birner, T., 2010: Residual circulation and tropopause structure. *J. Atmos. Sci.*, **67**, 2582–2600, doi:10.1175/2010JAS3287.1.
- Boer, G. J., and Coauthors, 1992: Some results from an intercomparison of the climates simulated by 14 atmospheric general circulation models. *J. Geophys. Res.*, **97** (D12), 12 771–12 786, doi:10.1029/92JD00722.
- Charlton-Perez, A. J., and Coauthors, 2013: On the lack of stratospheric dynamical variability in low-top versions of the CMIP5 models. *J. Geophys. Res. Atmos.*, **118**, 2494–2505, doi:10.1002/jgrd.50125.
- Chen, C.-C., and P. J. Rasch, 2012: Climate simulations with an isentropic finite-volume dynamical core. *J. Climate*, **25**, 2843–2861, doi:10.1175/2011JCLI4184.1.
- Czaja, A., and N. Blunt, 2011: A new mechanism for ocean-atmosphere coupling in midlatitudes. *Quart. J. Roy. Meteor. Soc.*, **137**, 1095–1101, doi:10.1002/qj.814.
- Dee, D. P., and Coauthors, 2011: The ERA-Interim reanalysis: Configuration and performance of the data assimilation system. *Quart. J. Roy. Meteor. Soc.*, **137**, 553–597, doi:10.1002/qj.828.
- Frierson, D. M. W., 2008: Midlatitude static stability in simple and comprehensive general circulation models. *J. Atmos. Sci.*, **65**, 1049–1062, doi:10.1175/2007JAS2373.1.
- , and N. A. Davis, 2011: The seasonal cycle of midlatitude static stability over land and ocean in global reanalyses. *Geophys. Res. Lett.*, **38**, L13803, doi:10.1029/2011GL047747.
- , I. M. Held, and P. Zurita-Gotor, 2006: A gray-radiation aquaplanet moist GCM. Part I: Static stability and eddy scale. *J. Atmos. Sci.*, **63**, 2548–2566, doi:10.1175/JAS3753.1.
- Held, I. M., 1982: On the height of the tropopause and the static stability of the troposphere. *J. Atmos. Sci.*, **39**, 412–417, doi:10.1175/1520-0469(1982)039<0412:OTHOTT>2.0.CO;2.

- Houghton, J. T., G. J. Jenkins, and J. J. Ephraums, Eds., 1990: *Climate Change: The IPCC Scientific Assessment*. Cambridge University Press, 410 pp.
- Hourdin, F., and Coauthors, 2013: LMDZ5B: The atmospheric component of the IPSL climate model with revisited parameterizations for clouds and convection. *Climate Dyn.*, **40**, 2193–2222, doi:10.1007/s00382-012-1343-y.
- John, V. O., and B. J. Soden, 2007: Temperature and humidity biases in global climate models and their impact on climate feedbacks. *Geophys. Res. Lett.*, **34**, L18704, doi:10.1029/2007GL030429.
- Johnson, D. R., 1997: “General coldness of climate models” and the second law: Implications for modeling the Earth system. *J. Climate*, **10**, 2826–2846, doi:10.1175/1520-0442(1997)010<2826:GCOOMA>2.0.CO;2.
- Juckes, M. N., 2000: The static stability of the midlatitude troposphere: The relevance of moisture. *J. Atmos. Sci.*, **57**, 3050–3057, doi:10.1175/1520-0469(2000)057<3050:TSSOTM>2.0.CO;2.
- Kanamitsu, M., W. Ebisuzaki, J. Woollen, S.-K. Yang, J. J. Hnilo, M. Fiorino, and G. L. Potter, 2002: NCEP-DOE AMIP-II Reanalysis (R-2). *Bull. Amer. Meteor. Soc.*, **83**, 1631–1643, doi:10.1175/BAMS-83-11-1631.
- Kang, S. M., I. M. Held, D. M. W. Frierson, and M. Zhao, 2008: The response of the ITCZ to extratropical thermal forcing: Idealized slab-ocean experiments with a GCM. *J. Climate*, **21**, 3521–3532, doi:10.1175/2007JCLI2146.1.
- , R. Seager, D. M. W. Frierson, and X. Liu, 2015: Croll revisited: Why is the Northern Hemisphere warmer than the Southern Hemisphere? *Climate Dyn.*, **44**, 1457–1472, doi:10.1007/s00382-014-2147-z.
- Kidston, J., and E. P. Gerber, 2010: Intermodel variability of the poleward shift of the austral jet stream in the CMIP3 integrations linked to biases in 20th century climatology. *Geophys. Res. Lett.*, **37**, L09708, doi:10.1029/2010GL042873.
- Korty, R. L., and T. Schneider, 2007: A climatology of the tropospheric thermal stratification using saturation potential vorticity. *J. Climate*, **20**, 5977–5991, doi:10.1175/2007JCLI1788.1.
- Pauluis, O., T. A. Shaw, and F. Laliberté, 2011: A statistical generalization of the transformed Eulerian-mean circulation for an arbitrary vertical coordinate system. *J. Atmos. Sci.*, **68**, 1766–1783, doi:10.1175/2011JAS3711.1.
- Reichler, T., and J. Kim, 2008: How well do coupled models simulate today’s climate? *Bull. Amer. Meteor. Soc.*, **89**, 303–311, doi:10.1175/BAMS-89-3-303.
- Saha, S., and Coauthors, 2010: The NCEP Climate Forecast System Reanalysis. *Bull. Amer. Meteor. Soc.*, **91**, 1015–1057, doi:10.1175/2010BAMS3001.1.
- Schaack, T. K., T. H. Zapotocny, A. J. Lenzen, and D. R. Johnson, 2004: Global climate simulation with the University of Wisconsin global hybrid isentropic coordinate model. *J. Climate*, **17**, 2998–3016, doi:10.1175/1520-0442(2004)017<2998:GCSWTU>2.0.CO;2.
- Schneider, T., 2004: The tropopause and the thermal stratification in the extratropics of a dry atmosphere. *J. Atmos. Sci.*, **61**, 1317–1340, doi:10.1175/1520-0469(2004)061<1317:TTATTS>2.0.CO;2.
- , 2007: The thermal stratification of the extratropical troposphere. *The Global Circulation of the Atmosphere*, T. Schneider and A. H. Sobel, Eds., Princeton University Press, 47–77.
- , and P. A. O’Gorman, 2008: Moist convection and the thermal stratification of the extratropical troposphere. *J. Atmos. Sci.*, **65**, 3571–3583, doi:10.1175/2008JAS2652.1.
- Son, S.-W., and Coauthors, 2010: Impact of stratospheric ozone on Southern Hemisphere circulation change: A multimodel assessment. *J. Geophys. Res.*, **115**, D00M07, doi:10.1029/2010JD014271.
- Taylor, K. E., R. J. Stouffer, and G. A. Meehl, 2012: An overview of CMIP5 and the experiment design. *Bull. Amer. Meteor. Soc.*, **93**, 485–498, doi:10.1175/BAMS-D-11-00094.1.
- Thuburn, J., and G. C. Craig, 2000: Stratospheric influence on tropopause height: The radiative constraint. *J. Atmos. Sci.*, **57**, 17–28, doi:10.1175/1520-0469(2000)057<0017:SIOTHT>2.0.CO;2.
- Wu, Y., and O. Pauluis, 2014: Midlatitude tropopause and low-level moisture. *J. Atmos. Sci.*, **71**, 1187–1200, doi:10.1175/JAS-D-13-0154.1.